Ferromagnetic Nanomaterials

DOI: 10.1002/anie.200905634

Scandium-Doped AlN 1D Hexagonal Nanoprisms: A Class of Room-Temperature Ferromagnetic Materials**

Weiwei Lei, Dan Liu, Yanming Ma, Xin Chen, Fubo Tian, Pinwen Zhu, Xiaohui Chen, Qiliang Cui,* and Guangtian Zou*

Dilute magnetic semiconductor (DMS) materials have been attracting intense interest for their potential applications in the field of spintronic devices because they combine charges and spins into a single-semiconductor medium.[1,2] DMS is usually produced by doping semiconductors with magnetic transition metals (TMs), such as Cr, Mn, Fe, Co, and Ni. Ferromagnetism in transition-metal-doped DMSs at or above room temperature has been observed.[3–6] However, the real origin of ferromagnetism is still not clear because magnetic transition metals are intrinsically magnetic and their precipitates or secondary magnetic phases in the host semiconductor may also contribute to the observed ferromagnetism. To avoid the problem of magnetic precipitates, fabricating new classes of DMS is highly desired. One approach is to dope semiconductors with intrinsically nonmagnetic elements. For example, copper, as a nonmagnetic element, has attracted theoretical and experimental attentions to produce ZnO- and GaN-based DMSs.[7–9] And it has been reported that carbon-doped ZnO materials are ferromagnetic above room temperature.[10] Another possible approach is to create intrinsic point defects in semiconductors, such as cation vacancies. Elfimov et al.[11] predicted by ab initio calculation that Ca vacancies in CaO prefer a ferromagnetic ground state. Recently, Pemmaraju and Sanvito[12] further predicted ferromagnetism for Hf vacancies in HfO_2 using the same method. However, the formation energy of such cation vacancies is so high that it is extremely difficult to obtain them in sufficiently high concentration under thermal equilibrium for utility.[13] Thus, viable and simple methods are highly desired for the synthesis of ferromagnetic semiconductors by reducing the formation energy of cation vacancies.

Recently, many efforts have been devoted to fabricating AlN-based DMS materials by making use of its wide bandgap (6.2 eV). Though magnetic transition metals, such as Mn, Cr, Co, and Fe, have been used to fabricate AlN-based DMS materials,[14–17] the question of the underlying ferromagnetism mechanism remains again largely unsolved. Earlier theoretical predictions suggested that Al vacancies could result in a ferromagnetic ground state with a magnetic moment of 3.0 μ_B.[18] However, they also predicted that it is hard to achieve a sufficiently high Al vacancy concentration in thermal equilibrium owing to the high formation energy of the vacancies. Herein, we report the first experimental fabrication of a DMS in AlN doped with a nonmagnetic rare-earth-element, scandium. Our first-principles calculations further demonstrated that the introduction of Sc into AlN significantly reduces the formation energy of Al vacancies and that the formation of this vacancy results in the ferromagnetic states. Such understandings are of great use in further exploring other DMS materials.

Figure 1a shows a scanning electron microscopy (SEM) image of typical AlN:Sc hexagonal nanoprisms. The AlN:Sc hexagonal nanoprisms scatter evenly and form a mesh. Interestingly, the AlN:Sc hexagonal nanoprisms from adjacent clusters try to approach each other, forming chains by self assembly (Figure 1b). These hexagonal nanoprisms have diameters around 80-100 nm and lengths around 150–180 nm. A typical chain-like structure is shown in Figure 1c. More

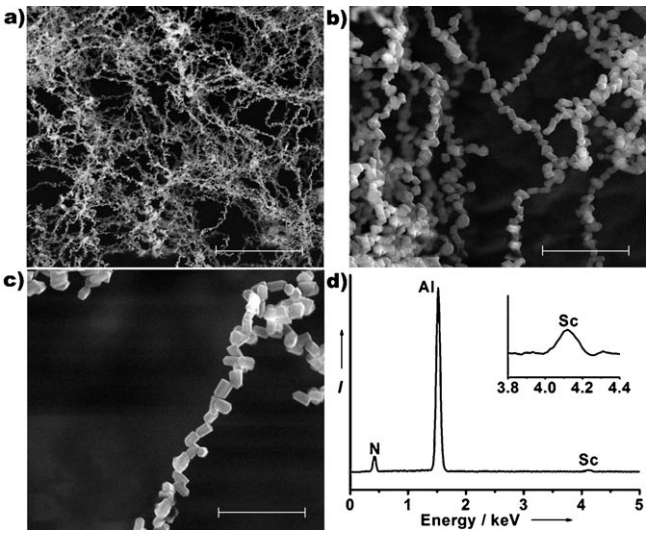

Figure 1. a) A low-magnification SEM image of the as-synthesized AlN:Sc hexagonal nanoprisms (scale bar: 5 μm). b) A medium-magnification SEM of the AlN:Sc hexagonal nanoprisms (scale bar: 1 μm). c) A high-magnification SEM image of typical AlN:Sc hexagonal nanoprisms with chainlike structure (scale bar: 500 nm). d) EDS spectrum of the as-synthesized AlN:Sc hexagonal nanoprisms.

[*] Dr. W. W. Lei, Dr. D. Liu, Prof. Y. M. Ma, Dr. X. Chen, Dr. F. B. Tian, Dr. P. W. Zhu, X. H. Chen, Prof. Q. L. Cui, Prof. G. T. Zou
State Key Laboratory of Superhard Materials
Jilin University, Changchun 130012 (China)
Fax: (+86) 431-85168346
E-mail: mym@jlu.edu.cn
cql@jlu.edu.cn

[**] The authors are grateful to Gehui Wen and Keh-Jim Dunn for many useful discussions. This work was supported by Natural Science Foundation of China (No. 50772043), The Post-graduate Innovative Foundation Program of Jilin University (20092003, 20091011, and MS20080217) and National Basic Research Program of China (Nos. 2005CB724400 and 2001CB711201).

Supporting information for this article is available on the WWW under http://dx.doi.org/10.1002/anie.200905634.

than 20 hexagonal nanoprisms can be assembled and form a micrometer-scale chain. Energy-dispersive X-ray spectroscopy (EDS) analysis (Figure 1d) reveals that the doping of Sc ions in AlN corresponds to a concentration close to 2.1%. Other impurity phases have not been detected.

Detailed structural characterization of the AlN:Sc hexagonal nanoprisms was performed by transmission electron microscopy (TEM) and high-resolution transmission electron microscopy (HRTEM). Figure 2a shows that the AlN:Sc nanoprisms exhibit predominantly hexagonal prism-like structure and stick together to form a chain. The hexagonal nanoprisms seem to have quite uniform shapes and sizes, free of impurity inclusions. A representative HRTEM image of a hexagonal nanoprism (Figure 2b) reveals that the hexagonal nanoprism has a single crystalline AlN:Sc wurtzite structure without any second phases, as corroborated by the corresponding selected area electron diffraction (SAED) pattern (inset in Figure 2b). The spacing of 0.521 nm measured from the lattice fringe corresponds to the *d*-spacing of the (0001) plane, suggesting a growth direction along the [0001] of the hexagonal nanoprism.

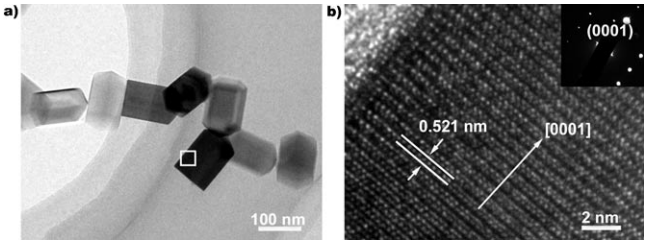

Figure 2. a) TEM image of the AlN:Sc hexagonal nanoprisms. b) HRTEM image of the area of the AlN:Sc hexagonal nanoprism highlighted in the square in (a). Inset: corresponding electron diffraction pattern.

A typical X-ray diffraction (XRD) pattern of the AlN:Sc hexagonal nanoprisms is shown in Figure 3. The diffraction peaks can be indexed to those of the wurtzite structure (space group: $P6_3mc$, No. 186) AlN (JCPDS file No. 08-0262). No diffraction peaks arising form ScN or Sc were observed in the XRD data. All peak positions of the AlN:Sc hexagonal nanoprisms are slightly shifted to lower angles relative to undoped AlN nanoparticles, suggesting an increase of lattice constants as a result of the substitution of larger radius Sc^{3+} ions ($r_{Sc} = 0.73$ Å) for the Al^{3+} ions ($r_{Al} = 0.51$ Å). A number of calculations show a clear increase in the lattice constants of the AlN after doping, resulting from dopant incorporation.[19,20]

The Raman spectra of the AlN:Sc hexagonal nanoprisms were obtained at room temperature. Hexagonal wurtzite AlN belongs to the $P6_3mc$ space group, with all the atoms occupying the C_{3v} sites. Six Raman-active modes are predicted by group theory: $1A_1(TO) + 1A_1(LO) + 1E_1(TO) + 1E_1(LO) + 2E_2$. Two distinct peaks centered at 608.6 cm^{-1} and 648.6 cm^{-1} correlate to the first-order vibrational modes of A_1(TO) and E_2(high), respectively, for AlN:Sc hexagonal nanoprisms (see Figure S1 in the Supporting Information). The slight red shift of E_2(high) and A_1(TO) of the AlN:Sc hexagonal nanoprisms relative to those of the undoped AlN nanoparticles, may be attributed to the disorder of the crystals resulting from the incorporation of Sc. Similar phenomena were observed in AlN:Cu nanorods.[21] This result further indicates that the Al cations (Al^{3+}) have been successfully substituted with Sc cations (Sc^{3+}), consistent with the XRD results. In addition, compared with undoped AlN nanoparticles, the vibrational mode E_1(TO) of AlN:Sc hexagonal nanoprisms is more pronounced. The high intensity of the E_1(TO) band of the AlN:Sc hexagonal nanoprisms probably resulted from the probing Raman bands of optical phonons in the *ab*-plane $\{10\bar{1}0\}$ facets,[22,23] because all of hexagonal nanoprisms have six prismatic *ab*-plane $\{10\bar{1}0\}$ facets and some of which lie on the substrate.

The plot of the magnetization (M) versus magnetic field strength (H), measured by a vibrating sample magnetometer (VSM) at 300 K (Figure 4), clearly indicates ferromagnetism at room temperature. The saturation magnetization and the coercive field of the AlN:Sc hexagonal nanoprisms are 0.049 emu g^{-1} and 299 Oe, respectively. Based on our XRD and HRTEM results, the formation of pure Sc metal and secondary phases, such as ScN and ScAl, has been safely ruled out. Since neither Al^{3+} nor Sc^{3+} ions are magnetic ions, the observed ferromagnetism is an intrinsic property of AlN:Sc.

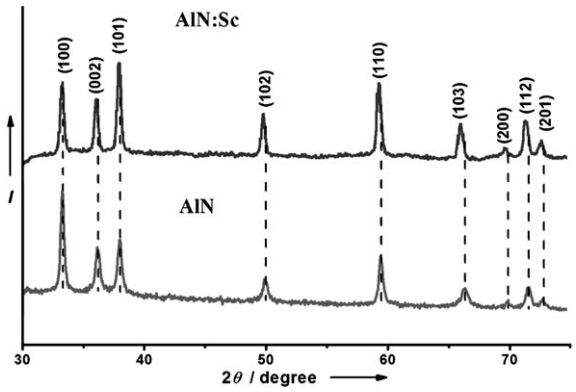

Figure 3. XRD pattern of AlN:Sc hexagonal nanoprisms (top) and undoped AlN nanoparticles (bottom).

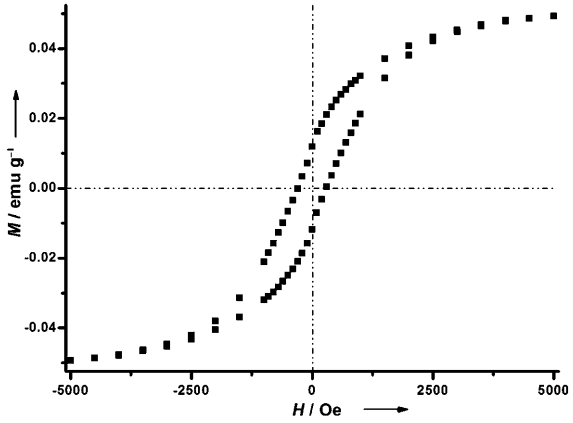

Figure 4. Magnetization hysteresis loop of the AlN:Sc hexagonal nanoprisms measured at room temperature.

We have performed first-principles calculations to understand the mechanism of the ferromagnetism in AlN:Sc hexagonal nanoprisms. Three $3\times3\times2$ supercell lattices each containing 72 atoms and large enough to study ferromagnetism[24] were constructed with: 1) one Al atom replaced by a Sc atom ($Al_{35}ScN_{36}$), 2) an Al vacancy created by removing one Al atom ($Al_{35}N_{36}$), and 3) one Al vacancy plus one substituting Sc atom ($Al_{34}ScN_{36}$). For the first system, the optimized lattice parameters slightly increase (e.g., an increase of 0.012 Å for a and 0.008 Å for c) relative to the undoped system, a change which can be attributed to the larger ionic radius of Sc than Al.[25,26] Our spin-polarized calculations did not reveal any magnetic behavior resulting from this introduction, as shown in the spin-resolved density of states in Figure 5a and the calculated total magnetic moment equals to zero as expected. For the second case (2), the majority spins and the minority spins are changed markedly around the Fermi level with the appearance of localized unoccupied bands (Figure 5b). It indicates that the Al vacancy induces a high spin polarization, which mainly arises from the unpaired 2p electrons of the nitrogen atoms around the vacancy site. The resulting total magnetic moment reaches $3.0\,\mu_B$, in good agreement with the results by Wu et al.[18] A similar mechanism, that an cation vacancy introduces magnetization to its neighboring anions, was reported also for the cases of CaO[11] and HfO_2.[12] For the third system (3), a nearly identical magnetic behavior to that in system (2) was identified (Figure 5c). Hence, the observed ferromagnetism in AlN:Sc hexagonal nanoprisms arises not from the Sc atom, but from the Al vacancies. However, it is worth noting that earlier theoretical predictions suggest a very high formation energy of Al vacancy and concluded the sufficient Al vacancy concentration would be hard to create under thermal equilibrium.[18] Therefore, it seems surprising that our experiments result in the formation of Al vacancies. As we will show below, the introduction of Sc into AlN is of great importance to effectively reduce the formation energy of the Al vacancy and makes it possible to fabricate a DMS in AlN.

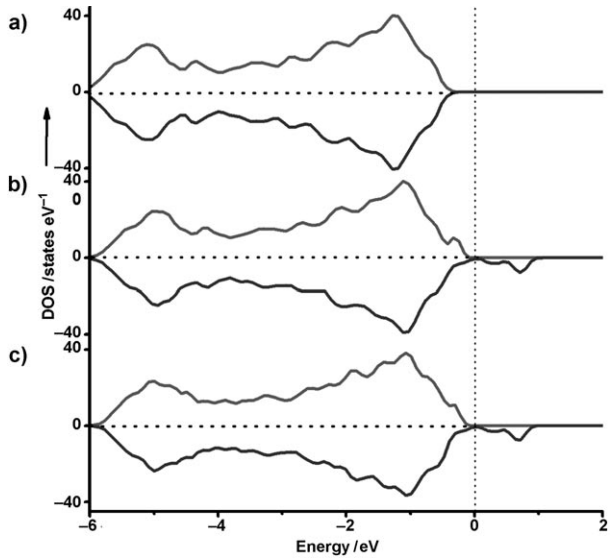

Figure 5. Spin-resolved density of states of a) the 72-atom AlN supercell with one Al atom substituted by a Sc atom; b) the 72-atom AlN supercell containing an Al vacancy; and c) the 72-atom AlN supercell containing an Al vacancy plus one substituting Sc atom. Fermi level is set to zero. Positive values correspond to the majority spin, negative values to the minority spin.

We have calculated the formation energies of systems (2) and (3). The defect formation energy in neutral state is defined as Equation (1)[18]

$$E^{f} = E^{tot}_{defect} - E^{tot}_{0} + n_{-}\mu_{-} - n_{+}\mu_{+} \quad (1)$$

where E^{tot}_{defect} is the total energy of the supercell containing the defect, $E^{tot}_{0}$is the total energy of the host supercell, n_{-} and n_{+} are the number of Al atoms substituted by the defect and the number of defect atoms introduced into the supercell, respectively, and $\mu_{-}$and μ_{+} are the corresponding chemical potentials. For the system of one Al vacancy, $n_{-}=n_{Al}=1$ and $n_{+}=0$, we calculated the formation energy of an Al vacancy (under nitrogen-rich conditions) to be 6.405 eV, in good agreement with that calculated by Wu et al.[18] This formation energy is so high that the formation of sufficient Al vacancies is hardly achieved at thermal equilibrium.[18] However, for the system of one Al vacancy plus one doped Sc atom, $n_{-}=n_{Al}=2$ and $n_{+}=n_{Sc}=1$, the calculated formation energy is 3.556 eV, much (ca. 2.849 eV) smaller than the system in the absence of Sc. These results suggest that the introduction of the Sc atom into AlN significantly reduces the formation energy of the Al vacancy.

The magnetic coupling between Al vacancies in the Sc-doped AlN supercell was also studied using the same approach as that used in the study of GaN.[24] We created two Al vacancies with a separation of 4.978 Å in the $3\times3\times2$ supercell by removing two Al atoms along the c direction. Total energy calculations are thus performed in ferromagnetic and antiferromagnetic states. The energy difference of the two systems is 181 meV, with the ferromagnetic state being the ground state. This result further confirms the ferromagnetic nature of Sc-doped AlN.

The remarkable experimental discovery of point defects in the ferromagnetism in pure HfO_2 film[27] has caused great interest in exploring new classes of DMSs. Since then, further experimental evidence on the observed ferromagnetism induced by point defects was found for ZnO, GaN, CdS, In_2O_3, and SnO_2 nanoparticles.[28–30] However, the observed magnetic moments are typically very small (10^{-3}–10^{-4} emu g^{-1}), which may be explained by the small quantity of cation or oxygen vacancies on the surface or subsurface of the DMSs. In addition, the theoretical studies on defect-induced magnetism in CaO and HfO_2 have predicted that the high cation-vacancy concentration on oxides is very unstable because of the high formation energy of the cation vacancies.[13,31] Our experimental results provided a viable method to obtain high defect concentration by doping nonmagnetic elements (e.g., Sc). The resulting magnetic moment (0.049 emu g^{-1}) is about one or two orders of magnitude larger than those in the above nanoparticles. The doping nonmagnetic element can significantly reduce the formation energy of cation vacancy and thereby induce the ferromag-

netic state. Exploring the new method to reduce the formation energy of cation vacancies would contribute to developing a new class of DMSs and bring a great opportunity to the field of spintronics.

In summary, we have demonstrated both experimentally and theoretically, that Sc-doped AlN hexagonal nanoprisms are ferromagnetic materials at room temperature with the typical diameter and length of 80–100 nm and 150–180 nm, respectively. Our first-principles calculations have established that the magnetism is caused by the formation of Al vacancies but not from the Sc dopant. Moreover, the calculated formation energy of an Al vacancy in AlN:Sc (3.556 eV) is much smaller than that in pure AlN (6.405 eV), implying that doping Sc has significantly reduced the formation energy of Al vacancies. These findings suggest a new approach in developing DMS.

Experimental Section

Single-crystalline AlN:Sc 1D hexagonal nanoprisms were synthesized in an improved arc discharge plasma setup.[32] Al (purity 99.99%), Sc (purity 99.99%), and N_2 gas (purity 99.99%) were used as sources. The N_2 pressure was 40 kPa. The input current was maintained at 100 A and the voltage was a little higher than 25 V. After reaction for 5 min, large numbers of white cotton-like solids deposited on the substrate. The morphology of the AlN:Sc hexagonal nanoprisms was characterized by field-emission scanning electron microscopy (SEM, XL 30 ESEM FEG) and high-resolution transmission electron microscopy (HRTEM, JEM-2100f). The chemical composition of these nanoprisms was determined by energy-dispersive X-ray spectroscopy (EDS). Micro-Raman spectroscopy was measured by Renishaw inVia (excited with an Ar^+ line at 514 nm). The crystal structures of AlN:Sc hexagonal nanoprisms were characterized by X-ray diffractometry (XRD, Rigaku D/Max-A, $Cu_{K\alpha}$). The magnetic properties were measured using a vibrating sample magnetometer (VSM) at room temperature.

We employed the all-electron projector augmented wave approach[33] within the Perdew-Burke-Ernzerhof parametrization of a generalized gradient approximation, as implemented in the Vienna ab initio simulation package code.[34] The plane-wave kinetic energy cutoff was set at 520 eV. The $4\times4\times3$ k-point meshes for the Brillouin zone sampling were constructed using the Monkhorst-Pack scheme.[35] The geometries of the supercells for various Sc dopings were fully optimized without using any symmetry constraints. For the relaxed structures, the atomic forces converged to be less than 0.02 eV $Å^{-1}$.

Received: October 8, 2009
Published online: November 26, 2009

Keywords: aluminum nitride · doping · magnetic properties · materials science · scandium

[1] P. Sharma, A. Gupta, K. V. Rao, F. J. Owens, R. Sharmaa, R. Ahuja, J. M. O. Guillen, B. Johansson, G. A. Gehring, *Nat. Mater.* **2003**, *2*, 673.
[2] H. Ohno, *Science* **1998**, *281*, 951.
[3] R. M. Frazier, G. T. Thaler, J. Y. Leifer, J. K. Hite, B. P. Gila, C. R. Abernathy, J. Pearton, *Appl. Phys. Lett.* **2005**, *86*, 052101.
[4] J. J. Liu, M. H. Yu, W. L. Zhou, *Appl. Phys. Lett.* **2005**, *87*, 172505.
[5] J. M. D. Coey, A. P. Douvalis, C. B. Fitzgerald, M. Venkatesan, *Appl. Phys. Lett.* **2004**, *84*, 1332.
[6] K. Ueda, H. Tabata, T. Kawai, *Appl. Phys. Lett.* **2001**, *79*, 988.
[7] L. H. Ye, A. J. Freeman, B. Delley, *Phys. Rev. B* **2006**, *73*, 033203.
[8] H. J. Xiang, S. H. Wei, *Nano Lett.* **2008**, *8*, 1825.
[9] H. K. Seong, J. Y. Kim, J. J. Kim, S. C. Lee, S. R. Kim, U. Kim, T. E. Park, H. J. Choi, *Nano Lett.* **2007**, *7*, 3366.
[10] H. Pan, J. B. Yi, L. Shen, R. Q. Wu, J. H. Yang, J. Y. Lin, Y. P. Feng, J. Ding, L. H. Van, J. H. Yin, *Phys. Rev. Lett.* **2007**, *99*, 127201.
[11] I. S. Elfimov, S. Yunoki, G. A. Sawatzky, *Phys. Rev. Lett.* **2002**, *89*, 216403.
[12] C. D. Pemmaraju, S. Sanvito, *Phys. Rev. Lett.* **2005**, *94*, 217205.
[13] J. Osorio-Guillén, S. Lany, S. V. Barabash, A. Zunger, *Phys. Rev. Lett.* **2006**, *96*, 107203.
[14] R. Frazier, G. Thaler, M. Overberg, B. Gila, C. R. Abernathy, S. J. Pearton, *Appl. Phys. Lett.* **2003**, *83*, 1758.
[15] D. Kumar, J. Antifakos, M. G. Blamire, Z. H. Barber, *Appl. Phys. Lett.* **2004**, *84*, 5004.
[16] R. M. Frazier, J. Stapleton, G. T. Thaler, C. R. Abernathy, S. J. Pearton, R. Rairigh, J. Kelly, A. F. Hebard, M. L. Nakarmi, K. B. Nam, J. Y. Lin, H. X. Jiang, J. M. Zavada, R. G. Wilson, *J. Appl. Phys.* **2003**, *94*, 1592.
[17] X. H. Ji, S. P. Lau, S. F. Yu, H. Y. Yang, T. S. Herng, A. Sedhain, J. Y. Lin, H. X. Jiang, K. S. Teng, J. S. Chen, *Appl. Phys. Lett.* **2007**, *90*, 193118.
[18] R. Q. Wu, G. W. Peng, L. Liu, Y. P. Feng, Z. G. Huang, Q. Y. Wu, *Appl. Phys. Lett.* **2006**, *89*, 142501.
[19] Y. Zhang, W. Liu, P. Liang, H. B. Niu, *Solid State Commun.* **2008**, *147*, 254.
[20] Y. Zhang, W. Liu, H. B. Niu, *Phys. Rev. B* **2008**, ***77***, 035201.
[21] X. H. Ji, S. P. Lau, S. F. Yu, H. Y. Yang, T. S. Herng, J. S. Chen, *Nanotechnology* **2007**, *18*, 105601.
[22] M. Bickermann, B. M. Epelbaum, P. Heimann, Z. G. Herro, A. Winnacker, *Appl. Phys. Lett.* **2005**, *86*, 131904.
[23] L. Bergman, M. Dutta, C. Balkas, R. F. Davis, J. A. Christman, D. Alexson, R. J. Nemanichc, *J. Appl. Phys.* **1999**, *85*, 3535.
[24] H. Jin, Y. Dai, B. B. Huang, M. H. Whangbo, *Appl. Phys. Lett.* **2009**, *94*, 162505.
[25] W. Jia, P. Han, M. Chi, S. Dang, B. S. Xu, X. G. Liu, *J. Appl. Phys.* **2007**, *101*, 113918.
[26] R. Q. Wu, G. W. Peng, L. Liu, Y. P. Feng, Z. G. Huang, Q. Y. Wu, *Appl. Phys. Lett.* **2006**, *89*, 062505.
[27] M. Venkatesan, C. B. Fitzgerald, J. M. D. Coey, *Nature* **2004**, *430*, 630.
[28] M. A. Garcia, J. M. Merino, E. Fernández Pinel, A. Quesada, J. de La Venta, M. L. Ruíz González, G. R. Castro, P. Crespo, J. Llopis, J. M. González-Calbet, A. Hernando, *Nano Lett.* **2007**, *7*, 1489.
[29] C. Madhu, A. Sundaresan, C. N. R. Rao, *Phys. Rev. B* **2008**, *77*, 201306(R).
[30] A. Sundaresan, R. Bhargavi, N. Rangarajan, U. Siddesh, C. N. R. Rao, *Phys. Rev. B* **2006**, *74*, 161306(R).
[31] J. Osorio-Guillen, S. Lany, S. V. Barabash, A. Zunger, *Phys. Rev. B* **2007**, *75*, 184421.
[32] W. W. Lei, D. Liu, J. Zhang, B. B. Liu, P. W. Zhu, T. Cui, Q. L. Cui, G. T. Zou, *Chem. Commun.* **2009**, 1365.
[33] P. E. Blöchl, *Phys. Rev. B* **1994**, *50*, 17953.
[34] G. Kresse, J. Heffner, *Phys. Rev. B* **1996**, *54*, 11169.
[35] H. J. Monkhorst, J. D. Pack, *Phys. Rev. B* **1976**, *13*, 5188.

